16TH EUROPEAN CONFERENCE ON EARTHQUAKE ENGINEERING THESSALONIKI 18 - 21 JUNE 2018

LOW-COST SEISMIC ISOLATOR FOR LOW-RISE BUILDINGS: EXPERIMENTAL TESTS

Ingrid E. Madera Sierra[1], Daniele Losanno[2], Mariacristina Spizzuoco[3], Johannio Marulanda[4], Peter Thomson[5]

ABSTRACT

Base isolation systems are one of the more commonly used technologies implemented around the world with the objective of protecting human lives and reducing damage to buildings during earthquakes. However, these systems are rarely used in emerging countries such as Colombia due to the relatively high costs. The development of fiber reinforced isolation systems with local technology eliminates importation costs of these devices, which is the principal obstacle for its massive use in Colombia. This paper describes the design and testing of a base isolation system for low-rise buildings, which represent over 70% of the construction projects in Colombia. Due to the lower costs and relatively simple fabrication process associated with such isolators, the proposed isolators are High Damping Rubber bearings (HDR). In the first phase, the main material properties, such as damping, effective stiffness, shear modulus and hardness, were fully characterized. Base on the mechanical test results, the appropriate rubber formulation and reinforcement material were selected. In the second phase, scale prototypes were tested in the Department of Industrial Engineering of the University of Naples Federico II, located in Naples-Italy, following the guidelines of FEMA 450. Specifically, shear and compression test on the prototype devices were carried out. The results show that the devices have great potential of being implemented as a low-cost isolation system.

Keywords: Base isolation; Low-cost isolator; Unbonded fiber reinforced isolator; High damping rubber bearing.

1. INTRODUCTION

Base isolation system is one of the more commonly used technologies implemented around the world with the objective of protecting human lives and reducing damage to buildings during earthquakes. The isolation system has been implemented in developed countries (Mason, 2015), and its effectiveness has been proved during different seismic events worldwide (Gómez, Marulanda, & Thomson, 2007). However, this system is rarely used in emerging countries, such as Colombia, due to their relatively high costs. The conventional devices used in the system are the steel reinforced isolators (SRIs), which are heavy and expensive; but, during the last few decades, new kinds of bearing reinforcement types for isolating purposes have been developed and investigated (Strauss, Apostolidi, Zimmermann, Gerhaher, & Dritsos, 2014). These new isolation devices contain fiber sheets rather than steel reinforcement within the bearing and are called fiber reinforced elastomeric isolators (FREIs). The main difference between SRIs and FREIs is that the last ones have the possibility to be used without connection to the structure, reducing cost, weight, installation and manufacturing process time. These characteristics allow the implementation of FREIs in any types of projects, such as residential buildings, not only in large and special ones.

Reducing the FREIs' cost can be met by replacing the natural rubber with recycled elastomers derived

[1]Magister in Civil Engineering, Universidad del Valle, Cali, Colombia, ingrid.madera@correounivalle.edu.co
[2]Ph. D in Civil Engineering, University of Naples, Federico II, Naples, Italy, dani.los@libero.it
[3]Ph. D in Civil Engineering, University of Naples, Federico II, Naples, Italy, spizzuoc@unina.it
[4]Ph. D in Civil Engineering, Universidad del Valle, Cali, Colombia, johannio.marulanda@correounivalle.edu.co
[5]Ph. D in Aerospace Engineering, Universidad del Valle, Cali, Colombia, peter.thomson@correounivalle.edu.co

from tires and industrial leftover, scrap tire rubber pads, and nanocomposite rubber (Spizzuoco, Calabrese, & Serino, 2014; Mishra, Igarashi, & Matsushima, 2013; Turer & Özden, 2008; Khanlari, Dehghani, Kokabi, & Razzaghi, 2010), or by using non-conventional materials such as carbon-fiber-reinforced plastic meshes, polyamide and engineering plastic sheets (Naghshineh, Akyuz, & Caner, 2015) (Bakhshi, Ali, Hosein, & Valadoust, 2011; Ping, y otros, 2014), or low-cost fiber mesh, like glass or nylon, instead carbon (bi-directional or quadri-directional fabrics) (Kang, Kang, & Moon, 2003; (Moon, Kang, Kang, Kim, & Kelly, 2003; Ashkezari, Aghakouchaka, & Kokabib, 2008; Kang & Kang, 2009) (Russo, Pauletta, & Cortesia, 2013; Strauss, Apostolidi, Zimmermann, Gerhaher, & Dritsos, 2014; Hedayati & Shahria, 2014b; Hedayati & Shahria, 2014a; Mordini & Strauss, 2008). Regarding the behavior, during horizontal displacements the corners of unbonded FREIs (U-FREIs) roll off the supports due to the unbonded condition and the lack of flexural rigidity of the fiber reinforcement. This eliminates the high tensile stress regions developed in a bonded isolator when it is displaced horizontally (Toopchi-Nezhad, Tait, & Drysdale, 2011; Van Engelen, Osgooei, Tait, & Konstantinidis, 2015). As such, the shear loads at the bearing contact surfaces are transferred through friction only.

The aim of this paper is to evaluate a novel U-FREI, proposed for low-rise residential buildings, which are the most common type of projects in the principal cities of Colombia. The devices were manufactured with materials and technology commercially available in Colombia, in an unbonded condition, without lead core and with a high damping rubber (HDR) matrix. As a reinforcement material, a polyester fiber mesh was proposed and compared with carbon one. The specimens were tested under compression, and shear and compression loads applied simultaneously, to determine their mechanical properties, such as stiffness and damping.

2. MECHANICAL CHARACTERIZATION OF THE RUBBER

In order to reduce the high weight and complex manufacturing process of low-damping natural rubber bearings with lead core, a high damping rubber bearing is proposed. For this device, a natural rubber compound with enough inherent damping, called high-damping natural rubber (HDR) was developed. The formulation, that is quantities and specifications of the matrix, filler, oil, vulcanizing agents, accelerants, temperature and mixing time, was chosen based on the results of the hardness and shear tests carried out on the rubber.

In the hardness test, the penetration resistance of the rubber was defined following the methodology of ASTM D2240 (ASTM International D2240, 1999), with a type A indenter (Figure 1a). The hardness obtained was 57, which is a typical value for rubber commonly used in engineered components (45-75A) (Gent, 2012) and in elastomeric bearings applications (Naeim & Kelly, 1999). Shear modulus and damping ratio of the rubber were defined with cyclic shear tests using four specimens conformed by two rubber samples vulcanized to steel plates, as shown in Figure 1b. The methodology used here was the one proposed by the ATC-17 (ATC-17, 1986).The specimens were subjected to shear deformation according to a triangular impulse, i.e. the maximum displacement in the rubber (D) was applied by increasing the shear deformation (γ_s) up to the value of 10%, 20%, 30%, 50%, 75%, 100%, 150%, 200%, 250% and 300%. In Table 1, the average values of the shear modulus (G) and damping ratio (β) are summarized for the range of deformations commonly used to design isolators for buildings applications. As expected, the material behaved as nonlinear at shear stresses less than 20%, with high modulus and damping; at strains higher than 100% the modulus was low and constant at 0.6MPa (Naeim & Kelly, 1999). Regarding damping, the value obtained (5.98%) is the minimum required (Madera Sierra, Losanno, Spizzuoco, Marulanda, & Thomson, 2017).

Table 1. Results of the cyclic shear tests. (Madera Sierra, Losanno, Spizzuoco, Marulanda, & Thomson, 2017)

γ_s=100%		γ_s=150%		γ_s=200%		γ_s=250%	
β [%]	G [MPa]	β [%]	G [MPa]	β [%]	G [MPa]	β [%]	G [MPa]
5.98	0.63	5.80	0.59	5.50	0.58	5.30	0.58

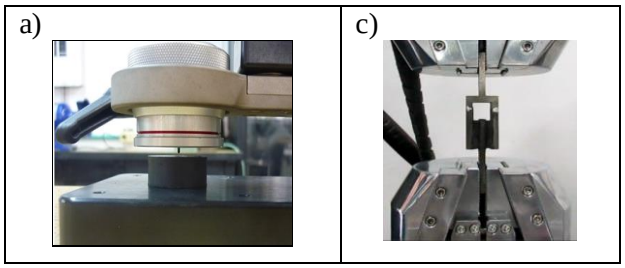

Figure 1. Experimental setup: a) hardness test, and b) shear test.

3. DESCRIPTION OF PROTOTYPES

The specimens were designed considering the properties of a benchmark building belonging to the Department of Structures for Engineering and Architecture (DiSt) at the University of Naples Federico II in Italy (Figure 2) (Calabrese, Spizzuoco, Serino, Della Corte, & Maddaloni, 2014), the FEMA450 requirements (Building Seismic Safety Council of the National Institute of Building Sciences (BSSC), 2003), the parameters developed by Naeim and Kelly (Naeim & Kelly, 1999) for unbonded applications, the characteristics for the ground motion of the site (Naples, Italy) and the mechanical properties of the materials. The structure is a steel frame with two degrees of freedom, having a total height of 2900mm and plan dimensions of 2650 × 2150 mm. The total weight of the structure is 7.7t, with a base level of 3.6t and a top level of 4.1t, for a total of 1.9t weight at the base of each column. A natural period of the building equal to $T_D = 1.15s$ was used to determinate the characteristics of the isolators.

Figure 2. Benchmark building.

The maximum design displacement (D_M) was calculated according to the maximum acceleration at the place under study (2.56m/s2). A design shear deformation equal to $\gamma_s = 100\%$ and a vertical pressure of 4.0MPa were considered. The total stiffness (K_{HTotal}) required was determined using the design period (T_D) and the total weight of the structure (W), by means of Equation 1, where g is the gravity. In order to design each device, this stiffness was divided by the total number of isolators.

$$K_{HTotal} = \frac{4\pi^2 W}{T_D^2 g} \tag{1}$$

Using D_M and γ_s, the total height of the rubber $H_r = \frac{D_M}{\gamma_s}$, was calculated. Then, with the stiffness required for each isolator (K), the isolator's area (A) was determined through Equation 2.

$$\boldsymbol{A = \frac{K_{HTotal} H_r A}{G}} \tag{2}$$

To investigate different flexible reinforcement alternatives, from both economical and functional points of view, two different materials were assessed with the same number of layers ($n_{f,s} = 14$): i) type 1 (T1), 1.1mm bidirectional polyester fiber fabric with elastic modulus of 1176MPa (Figure 3a) , and ii) type 2 (T2), 0.1mm bidirectional carbon fiber fabric with elastic modulus of 94666MPa (Figure 3b). Regarding the connections, the unbolted condition was assumed in both cases. In total, eight specimens were tested, two for each case type for two tests (Table 2).

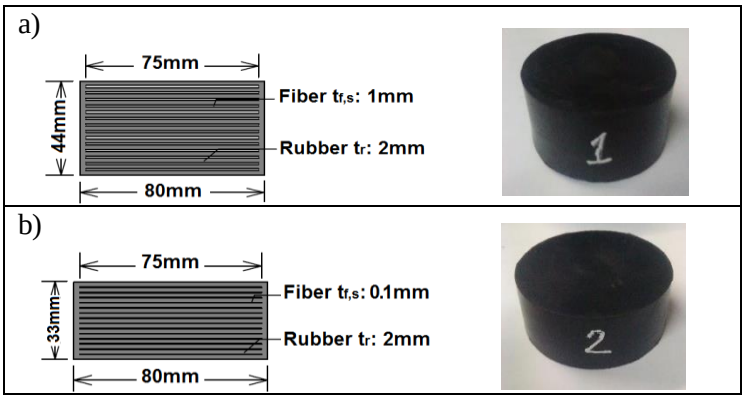

Figure 3. Cross section of the prototypes: a) T1 and b) T2. (Madera Sierra, Losanno, Spizzuoco, Marulanda, & Thomson, 2018).

Table 2. Types of isolators

Test	Prototype	Reinforcement	Specimen	Quantity	D [mm]	H [mm]	Reference
Compression - cyclic	T1	Polyester	A	1	78.4	43.8	T1A-1
			B	1	78.9	43.9	T1B-1
	T2	Carbon	A	1	79.3	34.3	T2A-1
			B	1	79.5	35.0	T2B-1
Shear	T1	Polyester	A	1	78.8	45.1	T1A-2
			B	1	78.5	43.6	T1B-2
	T2	Carbon	A	1	79.5	32.8	T2A-2
			B	1	79.6	32.7	T2B-2

4. EXPERIMENTAL TESTS

4.1 Compression test

The specimens were initially loaded monotonically, with a loading rate of 0.01 mm/s, until the design load $P = 19kN$; then, after a 1 minute pause, three fully reversed triangular cycles were applied at 0.05 mm/s with ±30% variation with respect to the design load. After a second pause of 1 minute, the specimens were monotonically unloaded with a loading rate of 0.01 mm/s (Figure 4a). The 1 minute pauses were needed to accommodate viscoelastic effects (Spizzuoco, Calabrese, & Serino, 2014). The compressive load was applied using a Humbolt HM-3000 Series Digital MasterLoader machine with capacity of 5.0t. The displacements were measured with inductive transducers (LVDT) with ±25mm of stroke and 0.01mm of precision (Figure 4b) (Madera Sierra, Losanno, Spizzuoco, Marulanda, & Thomson, 2018).

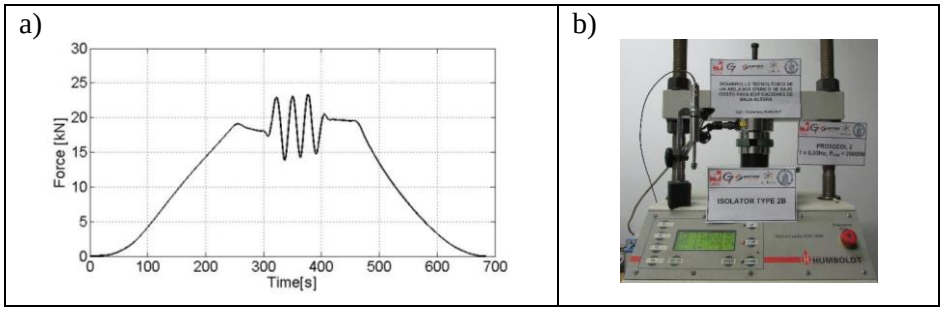

Figure 4. Cyclic compression test: a) protocol and b) setup. (Madera Sierra, Losanno, Spizzuoco, Marulanda, & Thomson, 2018).

4.2 Shear test

The specimens were tested using shear and compression loads, simultaneously. While they were loaded with 19kN force in the vertical direction, in the horizontal direction, two displacement protocols were applied. The first protocol was formulated considering the testing program of FEMA450 (Building Seismic Safety Council of the National Institute of Building Sciences (BSSC), 2003), which should be carried out on the isolators prior to the installation. For the second protocol, the deformation was increased until the expected maximum. The characteristics of each protocol are as follows:

- Protocol 1 (P1): it is composed by three parts. Part 1 consisted of three fully reversed cycles of loading at each level of displacement ($0.25D_M$, $0.50D_M$, $0.67D_M$, $1.00D_M$); in part 2 three fully reversed cycles of loading at the maximum displacement ($1.00D_M$) were applied; and in part 3 ten continuous fully reversed cycles of loading at 0.75 times the total maximum displacement ($0.75D_M$) were considered(Figure 5a) (Building Seismic Safety Council of the National Institute of Building Sciences (BSSC), 2003).
- Protocol 2 (P2): it is composed by the first part of protocol P1 and four fully reversed cycles the further displacement level ($1.50D_M$, $2.00D_M$, $2.50D_M$, $3.00D_M$). After this sequence, the devices were unloaded without a rest interval (Figure 5b). The same period of the cyclic shear tests on the rubber ($T_D = 1.15s$) was used.

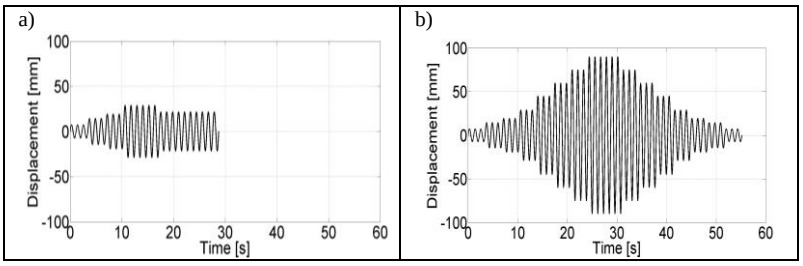

Figure 5. Displacement protocols for the shear tests: a) P1 and b) P2.

The correspondence between the percentage of D_M and γ_s is presented in Table 3.

Table 3. Equivalence between percentage of D_M and γ_s. (Madera Sierra, Losanno, Spizzuoco, Marulanda, & Thomson, 2018).

%D_M	**γ_s [%]**	**Displacement (d) [mm]**
0.25	25	7.2
0.50	50	14.5
0.67	67	19.4
0.75	75	21.7
1.00	100	29.0
1.50	150	43.5
2.00	200	58.0
2.50	250	72.5
3.00	300	87.0

The set up for the shear tests consisted of a compression machine with a shaking table driven by a horizontal hydraulic actuator that allowed to impose load or displacement histories, with maximum horizontal force capacity of 50 kN and maximum stroke of ±200 mm. A vertical hydraulic jack with capacity of 190 kN was used to apply the compression force. A dSPACE DS1103 controller board was

used for the real time control (Figure 6).

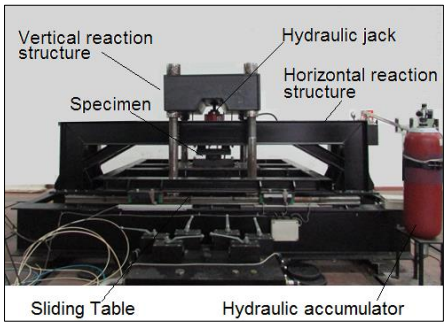

Figure 6. Shear test setup. (Madera Sierra, Losanno, Spizzuoco, Marulanda, & Thomson, 2017)

5. EXPERIMENTAL RESULTS

5.1 Compression test

In Figure 7, the force-displacement curves obtained from cyclic tests are shown. The vertical stiffness was calculated using the slope of the straight lines passing through the cyclic portions of the curves (Spizzuoco, Calabrese, & Serino, 2014) (
Table 4). In spite off the tension modulus of the carbon fiber is 80 times higher than the polyester one, the vertical stiffness of the prototypes with the last fiber was just 1.5 lower. This situation can be explained by the fact that the vertical stiffness is related with the modulus but also with the thickness of the mesh. The combination of both parameter allowed the polyester prototypes to achieve properties similar to the carbon fiber devices. The maximum displacements were similar in both cases, because at the beginning of the test the rubber acts alone while the fibers are tensioned, suffering a high initial deformation; after the fibers are reorganized and tensioned, the isolators are constrained and the deformations are minimized.

The experimental results were compared with the theoretical ones, with a maximum difference of 4% and 16% for polyester and carbon fibers, respectively. This similarity is because the cycles starting around the design load (±30%) and, in that point, the fibers are completely tensioned by confining the isolator and improving the vertical response. This situation represents the real condition of the isolators under seismic effects, because the devices are preloaded with the weight of the building when the earthquake starts, and this load may change around the maximum, being 30% a good estimation for this variation. For that reason, this test could be used to estimate the real response of the isolators during their service life.

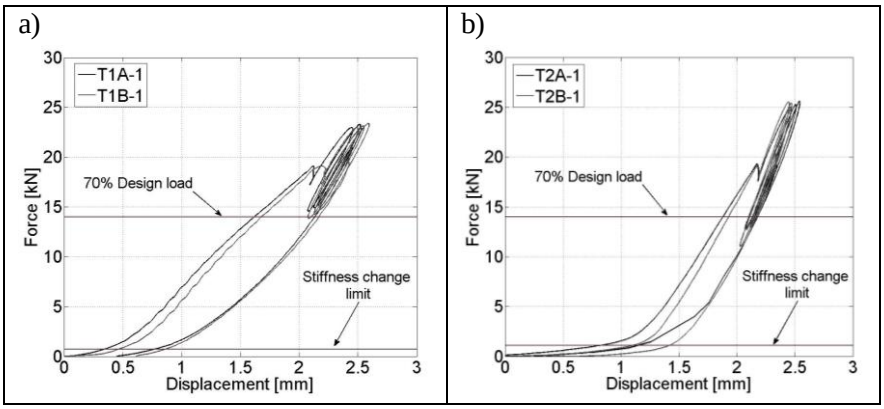

Figure 7. Force-displacement curves from cyclic compression tests: a) T1A-1, T1B-1 and b) T2A-1, T2B-1. (Madera Sierra, Losanno, Spizzuoco, Marulanda, & Thomson, 2018).

Table 4. Vertical stiffness – cyclic compression (Madera Sierra, Losanno, Spizzuoco, Marulanda, & Thomson, 2018).

		Kv [kN/mm]					Difference
Prototype	Specimen	Cycle 1	Cycle 2	Cycle 3	Average	Theoretical	[%]
T1	T1A-2	17	20	20	19	20	4.0
	T1B-2	20	20	20	20	20	0.3
T2	T2A-2	28	29	29	29	34	16.0
	T2B-2	31	32	31	31	34	8.0

Finally, the vertical and horizontal (K_H) stiffness ratio was calculated (Table 5). The last one was obtained from the design for the maximum displacement (D_M). For both type of isolators, the stiffness ratios were higher than the minimum required for the European Code (150), this could ensures a stable behavior of the isolator under vertical and horizontal loads.

Table 5. Vertical and horizontal stiffness ratio – cyclic compression

Prototype	Kv Average [kN/mm]	K_H Average [kN/mm]	Kv/ KH
T1	20	0.06	333
T2	30	0.05	600

5.2 Shear test

Prototypes T1b and T2a did not present any damage after the four protocols were applied. However, with prototypes T1a and T2b a failure was observed. In the T1a case, tearing of the cover part of the rubber occurred (Figure 8a), while in prototype T2b the failure occurred due to the delamination of the carbon and rubber layers (Figure 8b). This detachment may be produced by a deficient impregnation process when the adherence material was applied to the fibers. The flexibility of the reinforcement allowed the unbonded surfaces to roll off until the vertical faces touched the horizontal plates. After the originally vertical surfaces made contact with the horizontal support surfaces at high deformation levels (more than 200%), the prototypes showed a positive tangent stiffness and hardening behavior. This hardening is considered to be an advantage as it limits the maximum lateral displacement of the bearing and ensures the overall stability of the device for the maximum considered earthquake (MCE) (Toopchi-Nezhad, Tait, & Drysdale, Testing and modeling of square carbon fiber-reinforced elastomeric seismic isolators, 2008), (Naghshineh, Akyuz, & Caner, 2015).

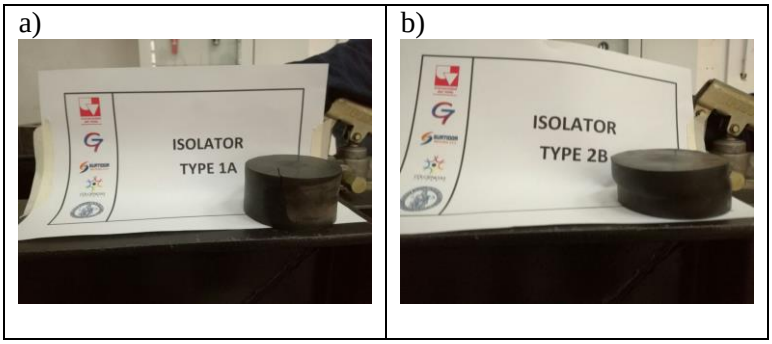

Figure 8. Failure modes of the prototypes: a) T1A-2, and b) T2B-2.

Through the shear tests, the hysteresis loops shown in Figure 9 were obtained. In all cases, a stiffness reduction with respect to the first cycles was observed for each deformation levels, due to the rupture of

the bonds among the polymer chains and the reinforcement particles (Mullins effect) (Van Engelen, Osgooei, Tait, & Konstantinidis, 2015). Also, the stiffness decreased after P1, then the isolators achieved a stable behavior (
Figure 10). This stress softening is related with the Mullins effect present in filled rubbers, as the used (Mullins, 1969). The resulting stiffness of T1 and T2 was similar, as expected, because both have the same area, rubber and connection condition. The main difference between T1 and T2 was the vertical stiffness, which influences the horizontal stiffness also. Although, the vertical stiffness of T2 is higher than the one of T1, in the horizontal direction this difference is lower. This is because the maximum vertical displacement at the design load in both cases is similar, due to the fact that the first part of the deformation is governed by the rubber acting alone while the reinforcement layers are tensioned.

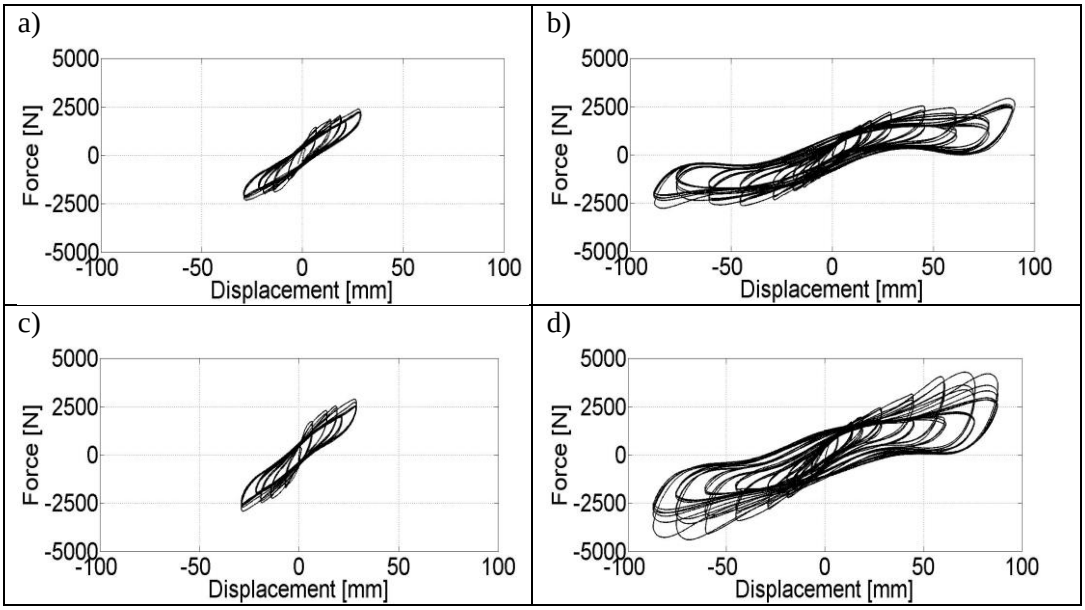

Figure 9. Hysteresis loops isolator: a) T1A-2-P1, b) T1A-2-P2, c) T2A-2-P1, and d) T2A-2-P2

As expected, in all cases the damping ratio was higher than the one obtained for the rubber only (Strauss, Apostolidi, Zimmermann, Gerhaher, & Dritsos, 2014), due to the interaction of the reinforcement with the rubber. In Table 6, the results for the main deformation levels of protocol 2 are summarized.

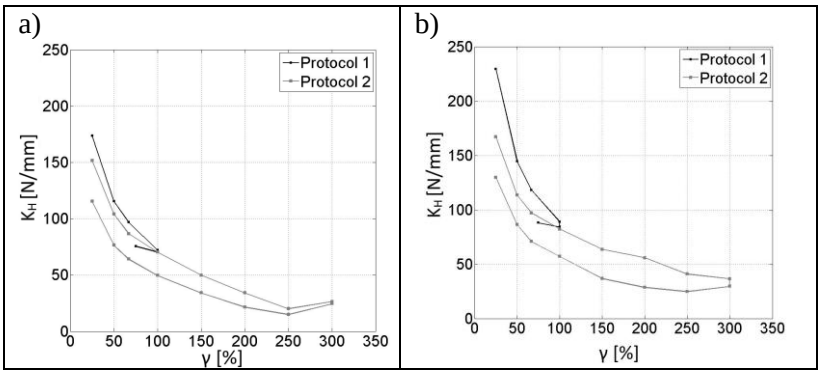

Figure 10. Horizontal stiffness (K_H) versus shear deformation (γ_s): a) T1A-2, and b) T2A-2

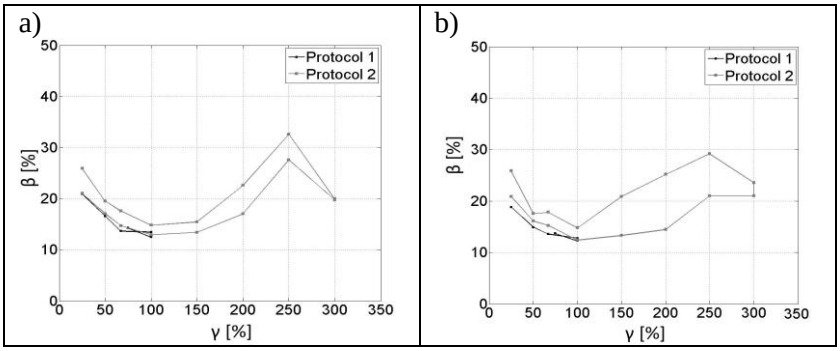

Figure 11. Damping ratio (β): a) T1A-2, and b) T2A-2.

Table 6. Isolator's properties for $\gamma_s = 100\%, 150\%, 200\%$ and 250%.

		γ_s=100%		γ_s=150%		γ_s=200%		γ_s=250%	
Type	Subtype	K_H [N/mm]	β [%]	K_H [N/mm]	β [%]	K_H [N/mm]	β [%]	K_H [N/mm]	β [%]
	a	70.3	12.9	49.9	13.4	34.1	17.0	20.0	27.6
1	b	72.0	11.6	51.8	12.7	33.9	17.0	26.7	21.2
	a	82.4	12.4	63.6	13.3	55.9	14.5	40.9	21.0
2	b	73.9	13.4	57.9	13.4	59.9	13.0	53.2	15.6

6. CONCLUSIONS

The combination of the tension modulus and thickness parameters allowed to the polyester prototypes to achieve a vertical stiffness in the same order of magnitude of the carbon fiber prototypes one. Also, in both cases was obtained the same maximum vertical displacement, due to the fact that, at the beginning the reinforcement does not constraint the rubber and the displacements in this stage are considerable; at the moment when the fibers start to act the additional displacement is minimum.

A satisfactory behavior of FREIs was obtained with both types of fiber in the horizontal direction, thanks to lower stress at the interface between different layers, achieving strain level up 250%, higher than the design strain (100%), without failed.

Both prototypes showed a positive tangent stiffness and hardening behavior after the originally vertical surfaces made contact with the horizontal support surfaces. This ensures the overall stability of the device against the maximum considered earthquake.

The results show high similarity between the vertical and horizontal properties for the isolators, satisfying with the minimum design values required in both cases. Nevertheless, taking account that the price of the polyester fiber is five times less than the carbon one, this is the option with higher potential to be implemented as a low-cost seismic isolation system in Colombia

7. ACKNOWLEDGMENTS

This research was financially supported by the grant P44842-020-2017 of the Administrative Department of Science and Technology of Colombia COLCIENCIAS and the Universidad del Valle through the Convocatoria 745-2016. The authors would like to acknowledge the scholarship for

Colombian doctoral formation No. 617 / 2013 provided by COLCIENCIAS and the collaboration of Prof. Giorgio Serino and Salvatore Strano from the Department of Structures for Engineering and Architecture, of the University of Naples, Federico II.

8. REFERENCES

Ashkezari, G. D., Aghakouchaka, A. A., & Kokabib, M. (2008). Design, manufacturing and evaluation of the performance of steel like fiber reinforced elastomeric seismic isolators. *Journal of materials processing technology, 197*(doi:10.1016/j.jmatprotec.2007.06.023), 140–150.

ASTM International D2240. (1999). *Standard Test Method for Rubber Property - Durometer Hardness.* United States: Annual Book of ASTM STANDARS.

ATC-17. (1986). *Quality Assurance and Control of Fabrication for a High-Damping-Rubber Base Isolation System.* San Francisco - California .

Bakhshi, Ali, Hosein, M., & Valadoust, V. (2011). Study on dynamic and mechanical characteristics of carbon fiber- and polyamide fiber-reinforced seismic isolators. *Materials and Structures*, 447–457.

Building Seismic Safety Council of the National Institute of Building Sciences (BSSC). (2003). *Recommended Provisions for Seismic Regulations for New Buildings and Other Structures FEMA 450.* Washington, D.C.

Calabrese, A., Spizzuoco, M., Serino, G., Della Corte, G., & Maddaloni, G. (2014). Shaking table investigation of a novel, low-cost, base isolation technology using recycled rubber. *Structural Control and Health Monitoring*, 1-16. doi:doi: 10.1002/stc.1663

Gent, A. N. (2012). *Engineering with rubber - How to design rubber components.* Munich, Germany: Hanser Publications.

Gómez, D., Marulanda, J., & Thomson, P. (2007). Sistemas de Control para la Protección de Estructuras Civiles Sometidas a Cargas Dinámicas. *Dyna*(155), 77-89.

Hedayati, F., & Shahria, M. (2014a). Sensitivity analysis of carbon fiber-reinforced elastomeric isolators based on experimental tests and finite element simulations. *Bulletin Earthquake Engineering, 12* (doi 10.1007/s10518-013-9556-y), 1025-1043.

Hedayati, F., & Shahria, M. (2014b). Performance of carbon fiber-reinforced elastomeric isolators manufactured in a simplified process: experimental investigations. *Structural Control and Health Monitoring, 21*(doi: 10.1002/stc.1653), 1347–1359.

Kang, B.-S., Kang, G.-J., & Moon, B.-Y. (2003). Hole and lead plug effect on fiber reinforced elastomeric. *Journal of Materials Processing Technology, 140*, 592–597.

Kang, G. J., & Kang, B. S. (2009). Dynamic analysis of fiber-reinforced elastomeric isolation structures. *Journal of Mechanical Science and Technology, 23* (DOI 10.1007/s12206-008-1214-y), 1132-1141.

Khanlari, S., Dehghani, G., Kokabi, M., & Razzaghi, M. (2010). Fiber-Reinforced nanocomposite seismic isolators: design and manufacturing. *Polymer Composites* (doi 10.1002/pc.20803), 299-306.

Madera Sierra, I. E., Losanno, D., Spizzuoco, M., Marulanda, J., & Thomson, P. (2017). Development and experimental behavior of HDR seismic isolators for low-rise residential buildings. *Engineering Structures Journal*, Under review.

Madera Sierra, I. E., Losanno, D., Spizzuoco, M., Marulanda, J., & Thomson, P. (2018). Experimental behavior of novel fiber reinforced isolators in unbounded configuration. *Soil Dynamics and Earthquake Engineering*, Submitted.

Mason, W. (2015). Seismic Isolation - The Gold Standard of Seismic Protection. *Structure Magazine*, 11-14.

Mishra, H. K., Igarashi, A., & Matsushima, H. (2013). Finite element analysis and experimental verification of the scrap tire rubber pad isolator. *Bulletin of Earthquake Engineering, 11* (doi: 10.1007/s10518-012-9393-4), 687–707.

Moon, B. Y., Kang, G. J., Kang, B. S., Kim, G. S., & Kelly, J. M. (2003). Mechanical properties of seismic isolation system with fiber-reinforced bearing of strip type. *International Applied Mechanics, 39* (doi:10.1023/B:INAM.0000010377.92594.3c), 133-142.

Mordini, A., & Strauss, A. (2008). An innovative earthquake isolation system using fibre reinforced rubber bearings. *Engineering Structures, 30* (doi:10.1016/j.engstruct.2008.03.010), 2739–2751.

Mullins, L. (1969). Softening of Rubber by Deformation. *Rubber Chemistry and Technology, 42*(1), 339-362.

Naeim, F., & Kelly, J. M. (1999). *Design of Seismic Isolated Structures from Theory to Practice.* New York , USA: John Wiley & Sons. Inc.

Naghshineh, A. K., Akyuz, U., & Caner, A. (2015). Lateral Response Comparison of Unbonded Elastomeric Bearings Reinforced with Carbon Fiber Mesh and Steel. *Shock and Vibration*.

Ngo, T. V., Deb, S. K., & Dutta, A. (2016). Effect of horizontal loading direction on performance of prototype square unbonded fibre reinforced elastomeric isolator. *Structural Control Health Monitoring*.

Ngo, T. V., Dutta, A., & Deb, S. (2017). Evaluation of horizontal stiffness of fibre-reinforced elastomeric isolators. *Earthquake Engineering & Structural Dynamics*.

Ping, T., Kai, X., Bin, W., ChiaMing, C., Han, L., & FuLin, Z. (2014). Development and performance evaluation of an innovative low-cost seismic isolator. *Science China Technological Sciences, 57* (doi: 10.1007/s11431-014-5662-6), 2050-2061.

Russo, G., Pauletta, M., & Cortesia, A. (2013). A study on experimental shear behavior of fiber-reinforced elastomeric isolators with various fiber layouts, elastomers and aging conditions. *Engineering Structures, 52* (http://dx.doi.org/10.1016/j.engstruct.2013.02.034), 422–433.

Spizzuoco, M., Calabrese, A., & Serino, G. (2014). Innovative low-cost recycled rubber–fiber reinforced isolator: Experimental tests and Finite Element Analyses. *Engineering Structures*, 99-111.

Strauss, A., Apostolidi, E., Zimmermann, T., Gerhaher, U., & Dritsos, S. (2014). Experimental investigations of fiber and steel reinforced elastomeric bearings: shear modulus and damping coefficient. *Engineering Structures, 75*, 402–413.

Toopchi-Nezhad, H. (2014). Horizontal stiffness solutions for unbonded fiber reinforced elastomeric bearings. *Structural Engineering and Mechanics*, 395-410.

Toopchi-Nezhad, H., Tait, M. J., & Drysdale, R. G. (2008). Testing and modeling of square carbon fiber-reinforced elastomeric seismic isolators. *Structural Control and Health Monitoring , 15*, 876–900.

Toopchi-Nezhad, H., Tait, M. J., & Drysdale, R. G. (2011). Bonded versus unbonded strip fiber reinforced elastomeric isolators: Finite element analysis. *Composite Structures, 93* (doi:10.1016/j.compstruct.2010.07.009), 850–859.

Turer, A., & Özden, B. (2008). Seismic base isolation using low-cost Scrap Tire Pads (STP). *Materials and Structures, 41* (doi 10.1617/s11527-007-9292-3), 891–908.

Van Engelen, N., Osgooei, P. M., Tait, M. J., & Konstantinidis, D. (2015). Partially bonded fiber-reinforced elastomeric isolators (PB-FREIs). *Structural Control and Health Monitoring, 22*, 417-432.